Electron Raman scattering in semiconductor quantum wire in an external magnetic field

2008 J. Phys.: Condens. Matter 20 045203

(http://iopscience.iop.org/0953-8984/20/4/045203)

J. Phys.: Condens. Matter **20** (2008) 045203 (7pp) doi:10.1088/0953-8984/20/04/045203

Electron Raman scattering in semiconductor quantum wire in an external magnetic field

Ri Betancourt-Riera[1], J M Nieto Jalil[1,2], R Riera[2], Re Betancourt-Riera[2] and R Rosas[3]

[1] Tenológico de Monterrey—Campus Sonora Norte, Bulevar Enrique Mazón López No. 965, CP 83000, Hermosillo, Sonora, Mexico
[2] Departamento de Investigación en Física, Universidad de Sonora, Apartado Postal 5-088, CP 83190, Hermosillo, Sonora, Mexico
[3] Departamento de Física, Universidad de Sonora, Apartado Postal 1626, CP 83000, Hermosillo, Sonora, Mexico

Received 24 May 2007, in final form 29 November 2007
Published 8 January 2008
Online at stacks.iop.org/JPhysCM/20/045203

Abstract
The differential cross-section for an electron Raman scattering process in a semiconductor quantum wire in the presence of an external magnetic field perpendicular to the plane of confinement is calculated. We assume a single parabolic conduction band. The emission spectra for different scattering configurations and the selection rules for the processes are studied. Singularities in the spectra are found and interpreted. The electron Raman scattering studied here can be used to provide direct information about the electron band and subband structure of these confinement systems. The magnetic field distribution is considered constant with value B_0 inside the wire and zero outside.

1. Introduction

The recent developments in nanometric fabrication techniques have made possible to obtain several nanostructures such as quantum wells, quantum dots, quantum wires, etc, which have allowed the development of new electronic devices and given rise to a revolution in electronics and optoelectronics. Basically, most of the physical properties presented by these nanostructures are implicitly contained in the wavefunction, and any change due to the confinement, or an external perturbation like the presence of a magnetic field, produces a change in the wavefunction which corresponds to a change in the physical properties of the system [1]. The application of an inhomogeneous magnetic field in these confined systems allowed us to obtain additional information about the behavior of the new subband structure mainly because of the confinement as well as the magnetic field, which gives rise to new optical, electronic and transport properties of the carriers in these systems [2–7].

Because of its precision, Raman scattering is a useful technique for studying the electronic structure of nanostructures, considering different polarizations of incident and emitted radiation [8–10]. Analysis of the differential cross-section of a Raman scattering process allows us to determine the subband structure of nanostructured systems by a direct inspection of the singularity positions in the spectra, considering the selection rules of transitions of the carriers participating in the interaction with different polarizations of the incident and emitted light. In general, the differential cross-section shows singularities related to intersubband and intraband transitions; in our case only intersubband transitions are considered. As it is shown, the result depends on the scattering configurations and the structure of singularities depends on the incident or emitted photon polarizations. The electron Raman scattering (ERS) in quantum well, quantum wire and quantum dot systems considering interband and intrasubband transitions with and without the participation of confinement phonons, but without the presence of an external magnetic field, has been studied in [11–16]; the case of a bulk semiconductor, considering the presence of electric and magnetic fields, was studied in [17–19].

We assume the electron confinement in the conduction band within a semiconductor quantum wire (QWW) at $T = 0$ K. The conduction band is considered parabolic, and it splits into a subband system due to the confinement and the presence of the magnetic field. The approximation of a parabolic band

is commonly used in the II–VI and III–V polar semiconductors when one works near to the center of the Brillouin zone in the reduced band scheme. Under these dynamic conditions the potential barriers do not imply interband transitions, so the nanostructures can be treated in the envelope function and effective mass approximations [11, 15].

Hashimzade *et al* [6] also calculated the interband electron Raman scattering in a quantum wire in a transverse magnetic field using a GaAs/AlAs matrix and a model which characterizes the quantum wire by a parabolic potential for electron–hole pairs. Their consideration of a magnetic field applied in the plane of the confinement gives selection rules different from those obtained in our work, because we have considered a magnetic field applied parallel to the axis of the wire.

In [9, 10] a theory of ERS for several low-dimensional structures was developed. In these cases, the conduction band was considered to be completely unoccupied, and for this reason the radiation field creates an electron–hole pair or an exciton by means of an electron interband transition involving the crystal valence and conduction bands. In this paper we consider that the conduction band is partially occupied; for this reason we have a confined electron in a QWW and therefore intersubband transitions can take place. This new situation was not considered for a QWW, although in [20, 21] similar systems were studied. When a carrier is present in the conduction band, the selection rules are the same for the transition associated with the emitted and incident radiation, which is different from the Raman scattering process mentioned above.

In this work we present a model of electron Raman scattering in a QWW in the presence of an external magnetic field. These systems can be fabricated from $GaAs/Al_{0.35}Ga_{0.75}As$ by using high-resolution electron-beam lithography techniques. The intersubband ERS processes can be qualitatively described in the following way: first an electron in the conduction band absorbs a photon of incident radiation of energy $\hbar\omega_l$, then the electron emits a photon of secondary radiation of energy $\hbar\omega_s$ due to a new intersubband transition [11].

2. Model and solution of Schrödinger's equation

The problem of determining the stationary states of an electron in a QWW system in the envelope function approximation leads to the solution of the Schrödinger equation. We consider a QWW of circular cross-section with radius ρ_0 and length L, which is in the presence of an external inhomogeneous magnetic field distribution in the z-direction. The distribution of the magnetic field, vector potential and confinement potential are given by:

$$\mathbf{B},\ \mathbf{A},\ V_c(\rho) = \begin{cases} B_0\mathbf{e}_z, & \frac{1}{2}B_0\hat{\mathbf{e}}_\theta, \quad 0; & 0 \leqslant \rho \leqslant \rho_0 \\ 0, & \dfrac{1}{2\rho}B_0^2\rho_0^2\hat{\mathbf{e}}_\theta, \quad V_0; & \rho_0 \leqslant \rho < \infty \end{cases}$$

where $\hat{\mathbf{e}}_z$ ($\hat{\mathbf{e}}_\theta$) is the unit vector in the z-direction (θ-direction). Notice that $\nabla \times \mathbf{A} = \mathbf{B}$ for $\rho \leqslant \rho_0$ and $\nabla \times \mathbf{A} = 0$ outside of the QWW. As required by this field distribution the following gauge $\nabla \cdot \mathbf{A} = 0$ is fulfilled. Then the Hamiltonian can be written as

$$\hat{H} = -\frac{\hbar^2}{2\mu}\nabla^2 + \frac{qA_\theta}{\mu c}\frac{L_z}{\rho} + \frac{q^2}{2\mu c^2}A_\theta^2 + V_c(\rho)$$

where μ is the electron effective mass, e the absolute value of charge of the electrons, A_θ the component θ of the magnetic vector potential associated with the magnetic field distribution and $L_z = -i\hbar\frac{\partial}{\partial\theta}$ the component z of the angular momentum.

The differential equation in each region of a QWW depends on the magnetic field distribution [2]. As is well known, the symmetry of the Hamiltonian allows the Schrödinger equation to be separable in cylindrical coordinates; therefore the total wavefunction has the following form

$$\Psi(\rho,\theta) = \frac{\exp\left[i(m\theta - k_z z)\right]}{\sqrt{2\pi L}}u_0(\rho) \times \begin{cases} A\exp\left(-\dfrac{x}{2}\right)x^{\frac{|m|}{2}}F(\beta, 1+|m|, x) & \rho \leqslant \rho_0 \\ BK_{|v|}\left(\dfrac{\gamma}{\rho_0}\rho\right) & \rho > \rho_0 \end{cases}$$

where

$$x = \frac{\rho^2}{2\rho_B^2}, \qquad \beta = -\frac{E_\rho}{\hbar\omega_0} + \frac{|m| - m + 1}{2}$$

$$v = m + \frac{\rho_0^2}{2\rho_B^2} \qquad \text{and} \qquad \gamma = \sqrt{\frac{2\mu_1}{\hbar^2}(V_0 - E_\rho)}$$

$u_0(\rho)$ is the electron Bloch function in the band and $m = 0, \pm1, \pm2, \ldots$ is the magnetic quantum number. $\omega_0 = \frac{eB_0}{\mu_2 c}$ is the cyclotron frequency, $\rho_B = \sqrt{\frac{\hbar}{\mu_2\omega_0}}$ is the confining magnetic length, F is the standard hypergeometric function and $K_{|v|}$ is the modified Bessel function of the second kind and order $|v|$. Considering the continuity of the wavefunction Ψ and the current density $\frac{1}{\mu}\frac{\partial\Psi}{\partial\rho}$ at the interface we can calculate the constants A and B; where μ_1 (μ_2) is the electron effective mass in the outside (inside) of the QWW.

Finally the electron energy for this system is

$$E_m(k_z) = E_\rho + \frac{\hbar^2}{2\mu}k_z^2 + \mu_B B_0 g^* m_s, \tag{1}$$

g^* is the Landé factor of the electron in the band, μ_B is the Bohr magneton and $m_s = \pm\frac{1}{2}$ for the two different spin states [22]. The electron energy due to the confinement, E_ρ, is obtained from the following secular equation

$$\mu_1 x_0 K_{|v|}\left(\frac{\gamma}{\rho_0}\rho\right)\left[\left(\frac{|m|}{x_0} - 1\right)F(\beta, 1+|m|, x_0) + F'(\beta, 1+|m|, x_0)\right] - \mu_2\gamma K'_{|v|}(\gamma) \times F(\beta, 1+|m|, x_0) = 0 \tag{2}$$

where $x_0 = \frac{\rho_0^2}{2\rho_B^2}$.

3. Raman cross-section

The differential cross-section for electron Raman scattering in a volume per unit solid angle for incoming light of frequency ω_l and scattered light of frequency ω_s is given by

$$\frac{d^2\sigma}{d\omega_s\, d\Omega} = \frac{V^2\omega_s^2\eta(\omega_s)}{8\pi^3c^4\eta(\omega_l)}W(\omega_s, \mathbf{e}_s) \tag{3}$$

where $\eta(\omega)$ is the refraction index as a function of the radiation frequency, $\mathbf{e}_s$ is the unit polarization vector for the emitted secondary radiation, c is the light velocity in a vacuum and $W(\omega_s, \mathbf{e}_s)$ is the transition rate for the emission of secondary radiation (with frequency ω_s and polarization $\mathbf{e}_s$) calculated according to Fermi's golden rule:

$$W(\omega_s, \mathbf{e}_s) = \frac{2\pi}{\hbar}\sum_f \left|\sum_a \frac{\langle f|\hat{H}_s|a\rangle\langle a|\hat{H}_l|i\rangle}{(\mathcal{E}_i - \mathcal{E}_a + i\Gamma_a)} + \sum_b \frac{\langle f|\hat{H}_l|b\rangle\langle b|\hat{H}_s|i\rangle}{(\mathcal{E}_i - \mathcal{E}_b + i\Gamma_b)}\right|^2 \delta(\mathcal{E}_f - \mathcal{E}_i) \tag{4}$$

$|i\rangle$ and $|f\rangle$ are the initial and final states with energies $\mathcal{E}_i$ and $\mathcal{E}_f$, $|a\rangle$ and $|b\rangle$ are the intermediate states with energies $\mathcal{E}_a$ and $\mathcal{E}_b$, and Γ_a and Γ_b are the lifetimes [11, 14]. The second terms of equation (4) are the so-called interference diagrams

$$\sum_b \frac{\langle f|\hat{H}_l|b\rangle\langle b|\hat{H}_s|i\rangle}{(\mathcal{E}_i - \mathcal{E}_b + i\Gamma_b)}.$$

In previous works [12, 16] the contribution of the interference diagrams was neglected because the gap was larger than the band offset of the electron–hole pairs [9]. In the present work these terms must be considered because they do affect the excitation spectra; however, the information given by the excitation spectra is similar to that from the emission spectra, therefore a corresponding graph was not included.

The Hamiltonian operator for the radiation field has the form

$$\hat{H}_r = \frac{|e|}{\mu}\sqrt{\frac{2\pi\hbar}{V\omega_r}}\left(\mathbf{e}_r\cdot\hat{\mathbf{p}}\right), \qquad \hat{\mathbf{p}} = -i\hbar\nabla, \tag{5}$$

where $\hat{H}_r$ is in the dipole approximation with frequency ω_r, and $\mathbf{e}_r$ is the light polarization unit vector; the subindex $r = l(s)$ indicates the incident (secondary) radiation. The dipole approximation is commonly used in electron Raman scattering and resonant Raman scattering in nanostructures [9–16]. This approximation is valid as long as the radiation wavelength is much larger than the radius of the wire. In this work we have considered that the radius of wire is less than 100 Å. The effect of reduced dimensionality on the free carrier absorption and the selection rules for intersubband transition have been discussed in [9], and there it is shown that the ERS can only take place in the confinement direction.

For the calculation of the differential cross-section given by equation (3) we need to calculate the matrix elements appearing in equation (4). For the case of the radiation field we use the condition $\mathbf{k}_z = 0$ [15]; thus, by considering the equation (5) and the wavefunction corresponding to a QWW the following matrix elements are obtained:

$$\langle\Psi'|\hat{H}_r|\Psi''\rangle_\pm = -i\hbar\frac{|e|}{\mu_0}\sqrt{\frac{2\pi\hbar}{V\omega_r}}\frac{\mathbf{e}_r\cdot\mathbf{e}_\pm}{\rho_0}T_\pm\left(m', m''\right), \tag{6}$$

where

$$T_\pm\left(m', m''\right) = \rho_0\left[\frac{\mu_0}{\mu_1}\langle\Psi'_{\text{outside}}|\nabla_\pm|\Psi''_{\text{outside}}\rangle + \frac{\mu_0}{\mu_1}\langle\Psi'_{\text{inside}}|\nabla_\pm|\Psi''_{\text{inside}}\rangle\right], = \left[\mathrm{I}_{m',m''} \pm m''\mathrm{II}_{m',m''}\right]\delta_{m'\pm1,m''}\delta_{k'_z,k''_z}$$

μ_0 is the free electron mass and $\nabla_\pm = \frac{\exp(\pm i\theta)}{\sqrt{2}}\left(\frac{\partial}{\partial\rho} \pm \frac{i}{\rho}\frac{\partial}{\partial\theta}\right)$. The explicit form of $\mathrm{I}_{m',m''}$ and $\mathrm{II}_{m',m''}$ is very complicated and their expressions can be calculated following the method reported in [16]. As can be observed, the emission or absorption of one photon can only take place between consecutive states of the quantum number m, according to the selection rules $m'' = m' \pm 1$.

In the initial state we have an electron in a conduction subband and an incident radiation photon; for the final state we have an electron in the other conduction subband and a secondary radiation photon:

$$\mathcal{E}_i = \hbar\omega_l + E_{m''}(k_z) \qquad \text{and} \qquad \mathcal{E}_f = \hbar\omega_s + E_m(k_z). \tag{7}$$

For the intermediate states, we have two possibilities [11]: (a) the electron absorbs the incident photon and later emits the secondary radiation photon or (b) the electron emits the secondary radiation photon and later absorbs the incident photon, then we can write

$$\mathcal{E}_a = E_{m'}(k_z) \qquad \text{and} \qquad \mathcal{E}_b = \hbar\omega_l + \hbar\omega_s + E_{m'}(k_z). \tag{8}$$

Using equations (1)–(8) we obtain four different contributions to the DCS, depending on the polarization of the incident and emitted radiation; finally we can write the differential cross-section as:

$$\left[\frac{d^2\sigma}{d\omega_s d\Omega}\right]_{\pm\pm} = \frac{\eta(\omega_s)}{\eta(\omega_l)}\left(\frac{e}{c}\right)^4\frac{\hbar}{\pi\mu_0^2\rho_0}\frac{\omega_s}{\omega_l}\Gamma_f\left(\sigma_s^\pm\cdot\sigma_l^\pm\right)^2 \times\sum_{n,n''}\sum_m\frac{|M_{\pm\pm}|^2}{[\hbar\omega_l - \hbar\omega_s + E_\rho(m+2, n'') - E_\rho(m, n)]^2 + \Gamma_f^2}, \tag{9}$$

and

$$\left[\frac{d^2\sigma}{d\omega_s\, d\Omega}\right]_{\pm\mp} = \frac{\eta(\omega_s)}{\eta(\omega_l)}\left(\frac{e}{c}\right)^4\frac{\hbar}{\pi\mu_0^2\rho_0}\frac{\omega_s}{\omega_l}\Gamma_f\left(\sigma_s^\pm\cdot\sigma_l^\mp\right)^2 \times\sum_{n,n''}\sum_m\frac{|M_{\pm\mp}|^2}{\left[\hbar\omega_l - \hbar\omega_s + E_\rho(m, n'') - E_\rho(m, n)\right]^2 + \Gamma_f^2} \tag{10}$$

where

$$M_{\pm\pm} = \frac{\hbar^2}{2\mu_0\rho_0^2}\sum_{n'}T_\pm(m, m\pm1)\,T_\pm(m\pm1, m\pm2) \times\left[\frac{1}{\hbar\omega_s + E_\rho(m, n) - E_\rho(m\pm1, n') + i\Gamma_{a'}} - \frac{1}{\hbar\omega_l - E_\rho(m, n) + E_\rho(m\pm1, n') - i\Gamma_{b'}}\right], \tag{11}$$

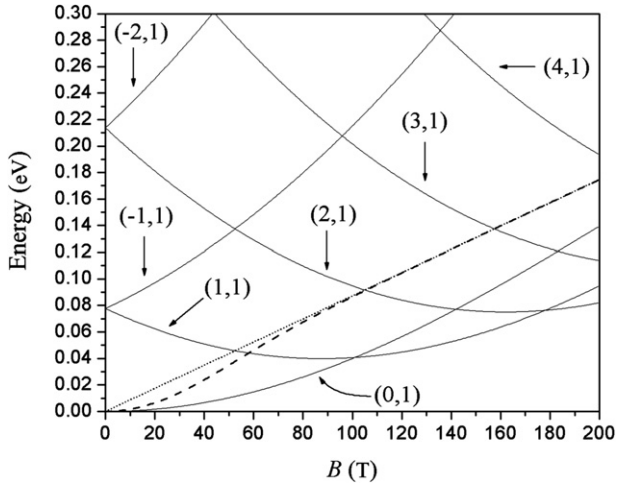

Figure 1. The electron states for a QWW. The solid line corresponds to the electron state for $\rho_0 = 50$ Å, the dashed line to the electron state (0, 1) for $\rho_0 = 100$ Å and the dotted line to $\frac{\hbar\omega_0}{2}$.

$$M_{\pm\mp} = \frac{\hbar^2}{2\mu_0\rho_0^2}\sum_{n'} T_{\pm}(m, m\pm1)\, T_{\mp}(m\pm1, m) \times\left[\frac{1}{\hbar\omega_s + E_\rho(m,n) - E_\rho(m\pm1,n') + i\Gamma_a} - \frac{1}{\hbar\omega_l - E_\rho(m,n) + E_\rho(m\pm1,n') - i\Gamma_b}\right], \tag{12}$$

$\sigma_r^{\pm} = \mathbf{e}_r \cdot \mathbf{e}_{\pm}$ and n is the order of the zero of equation (2).

4. Results and conclusions

We have calculated the differential cross-section for an intersubband ERS process in a semiconductor quantum wire with a magnetic field and from our results it can be observed that four independent contributions to the differential cross-section exist. The physical parameters used in our formulae correspond to a system grown in a $GaAs/Al_{0.35}Ga_{0.65}As$ matrix: $V_0 = 0.3$ eV, $\mu_1 = 0.096\ \mu_0$, $\mu_2 = 0.0665\ \mu_0$ and $\Gamma_a = \Gamma_b = \Gamma_f = 0.001$ eV [23].

In figure 1 we can observe the electron state energies for a QWW. The unfolding of energy levels due to the magnetic field is shown, breaking the degeneration for the m quantum number. The *gap* between the (m, n) and $(-m, n)$ states increases with increase in the intensity of the magnetic field. We also can observe the confinement effect in the magnetic field ground state ($\frac{\hbar\omega_0}{2}$). With increasing magnetic field the effect of the confinement diminishes and it practically disappears when $B = 100$ T. It is clear from the figure that there is no crossing between states with $m < 0$, whereas for states with $m > 0$ the opposite occurs, which is because the increase in m produces an increment of the *gap* between the (m, n) and $(-m, n)$ states. It is interesting to observe how the increase in the intensity of the magnetic field is able to 'take out' from the QWW some levels for $m < 0$ like $(-1, 1)$ and $(-2, 1)$ and to introduce some levels for $m > 0$ like (3, 1) and (4, 1).

The equations (9) and (10) have peaks when

$$\hbar\omega_r(m\pm1, n', m, n) \to \hbar\omega_r = E_\rho(m\pm1, n') - E_\rho(m, n)$$

and

$$\hbar\omega(m+\alpha, n'', m, n) \to \hbar\omega_r = \begin{cases} \hbar\omega_s - E_\rho(m+\alpha, n'') + E_\rho(m, n); & r = l \\ \hbar\omega_l + E_\rho(m+\alpha, n'') - E_\rho(m, n); & r = s \end{cases}$$

with $\alpha = 2$ for $[\sigma_s^{\pm}\cdot\sigma_l^{\pm}]$ polarization and $\alpha = 0$ for $[\sigma_s^{\pm}\cdot\sigma_l^{\mp}]$ polarization.

As can be observed, the magnetic field produces the level splits in two different states, which is due to the fact that the transition can only occur between consecutive states for the quantum number m, i.e. $m' = m \pm 1$, but there is no restriction for the quantum number n. For this reason we cannot observe peaks related to intrasubband transition. We have obtained two types of peak because we had two different subband systems, one for the negative values of m and another for the positive ones. The contact between the subband system is in this case the state $m = 0$, $n = 1$; this level corresponds to the magnetic field ground state. The selection rules are different for the four polarizations, and we have the transitions

$$[\sigma^-, \sigma^-](m-1, n') \to (m, n)$$

$$[\sigma^-, \sigma^+](m-1, n') \to (m, n)$$

$$[\sigma^+, \sigma^+](m+1, n') \to (m, n)$$

$$[\sigma^+, \sigma^-](m+1, n') \to (m, n).$$

The peaks associated with these transitions are independent of the incident photon for the emission spectra and independent of the secondary photon for the excitation spectra. In some previous works they were named as resonant peaks [11, 13–15]. The other peaks are characteristic of the excitations of the system attributed to inter-magneto-subband single-electron excitation and are related with the following transitions:

$$[\sigma^-, \sigma^-](m-2, n'') \to (m, n)$$

$$[\sigma^-, \sigma^+](m, n) \to (m, n)$$

$$[\sigma^+, \sigma^+](m+2, n'') \to (m, n)$$

$$[\sigma^+, \sigma^-](m, n) \to (m, n).$$

These transitions are responsible for the increment, approximately one order of magnitude, of the Raman spectra intensity for $[\sigma^-, \sigma^+]$ and $[\sigma^+, \sigma^-]$ polarizations, (see figure 2).

In figure 2 the emission spectrum for different polarizations of the incident and secondary photon is shown, with $\rho_0 = 50$ Å and $\hbar\omega_l = 0.28$ eV. The magnetic field causes the appearance of new levels which produces new peaks that were not observed in the previous figure. Here we can observe that the magnetic field moves the peak of polarizations $[\sigma_s^-\cdot\sigma_l^-]$

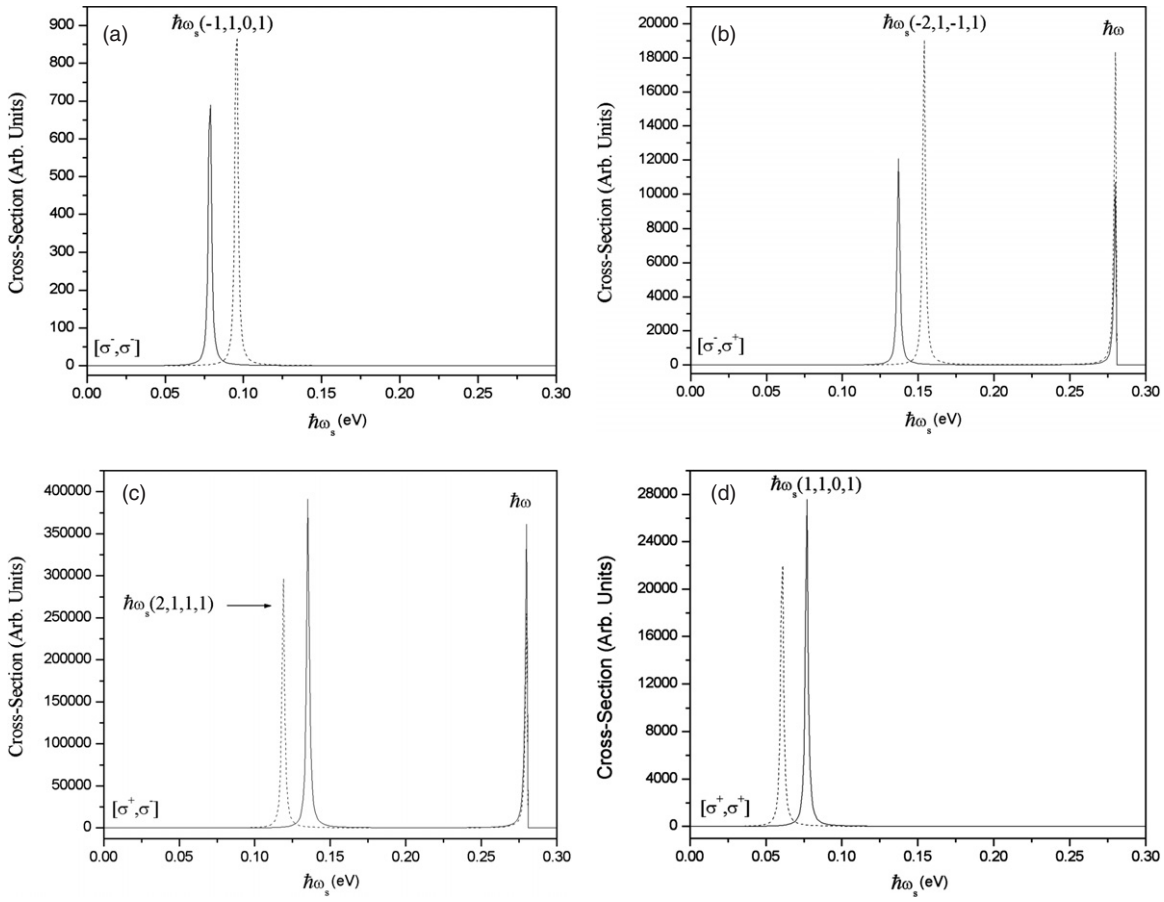

Figure 2. The emission spectra for a QWW for $\rho_0 = 50$ Å and $\hbar\omega_l = 0.28$ eV. The solid line corresponds to $B_0 = 1$ T and the dashed line to $B_0 = 20$ T: (a) $[\sigma_s^- \cdot \sigma_l^-]$; (b) $[\sigma_s^- \cdot \sigma_l^+]$; (c) $[\sigma_s^+ \cdot \sigma_l^+]$ and (d) $[\sigma_s^+ \cdot \sigma_l^-]$.

and $[\sigma_s^- \cdot \sigma_l^+]$ to bigger energy values, whereas for the polarizations $[\sigma_s^+ \cdot \sigma_l^+]$ and $[\sigma_s^+ \cdot \sigma_l^-]$ the peaks are displaced to lower energy values. This behavior is due to the increase in the *gap* between the negative subbands and the decrease in the *gap* between the positive subbands with increasing magnetic field. In polarizations $[\sigma_s^- \cdot \sigma_l^-]$ and $[\sigma_s^+ \cdot \sigma_l^+]$ the peak corresponding to $\hbar\omega$ is not observed; this transition only takes place in the $[\sigma^-, \sigma^+]$ and $[\sigma^+, \sigma^-]$ polarizations due to the selection rules (see equations (11) and (12)).

In figure 3 the radius increases from 50 to 60 Å for $B_0 = 1.0$ T. The result is the appearance of new peaks, because the increased radius allows the appearance of new subbands inside the QWW. We can also observe that the peaks obtained for 50 Å remain but they are displaced to lower energy values, because the increased radius causes a decrease in the *gap* between the subbands. These results are different from those obtained previously in [5, 12, 16], because in these calculations the conduction band was considered empty. By comparing figures 2 and 3 we can conclude that the intensities of the peaks obtained from transitions in the positive subband are bigger than the intensities of the peaks obtained from transitions in the negative subband; this happens because the magnetic field diminishes the separation between the positive levels and increases the separation between the negative ones.

The electron Raman scattering used in our work only considers intraband transitions because the conduction bands are partially occupied, as it corresponds to a system grown in a $GaAs/Al_{0.35}Ga_{0.65}As$ matrix. On the other hand, interband electron Raman scattering is possible in two different processes: interband electron Raman scattering with the intermediate state in the conduction band, and the intermediate state in the valence band. These processes are possible because in the GaAs/AlAs quantum wire [6] the conduction band is empty and the valence band is completely occupied by electrons, and for this reason the creation of electron–hole pairs or excitons by interband transitions is required.

The structure of the differential cross-section, as given in the figures, provides a transparent understanding of the energy subband structure of QWW in the presence of a magnetic field. In summary, we have presented a formalism for the calculation of the Raman differential cross-section for an ERS in a semiconductor quantum wire considering an inhomogeneous magnetic field distribution and have obtained the selection rules for this process.

The main feature of the ERS is the appearance of a rich spectrum with many frequencies, due to the non-equidistant electron energy levels and the presence (absence) of a selection rule for transitions involving changes of the m (n) quantum number. The dependence of the differential cross-section on the size of the QWW and the magnetic field could be used for spectroscopic characterization of such systems. Let us finally remark that in this work we have applied a simplified model for

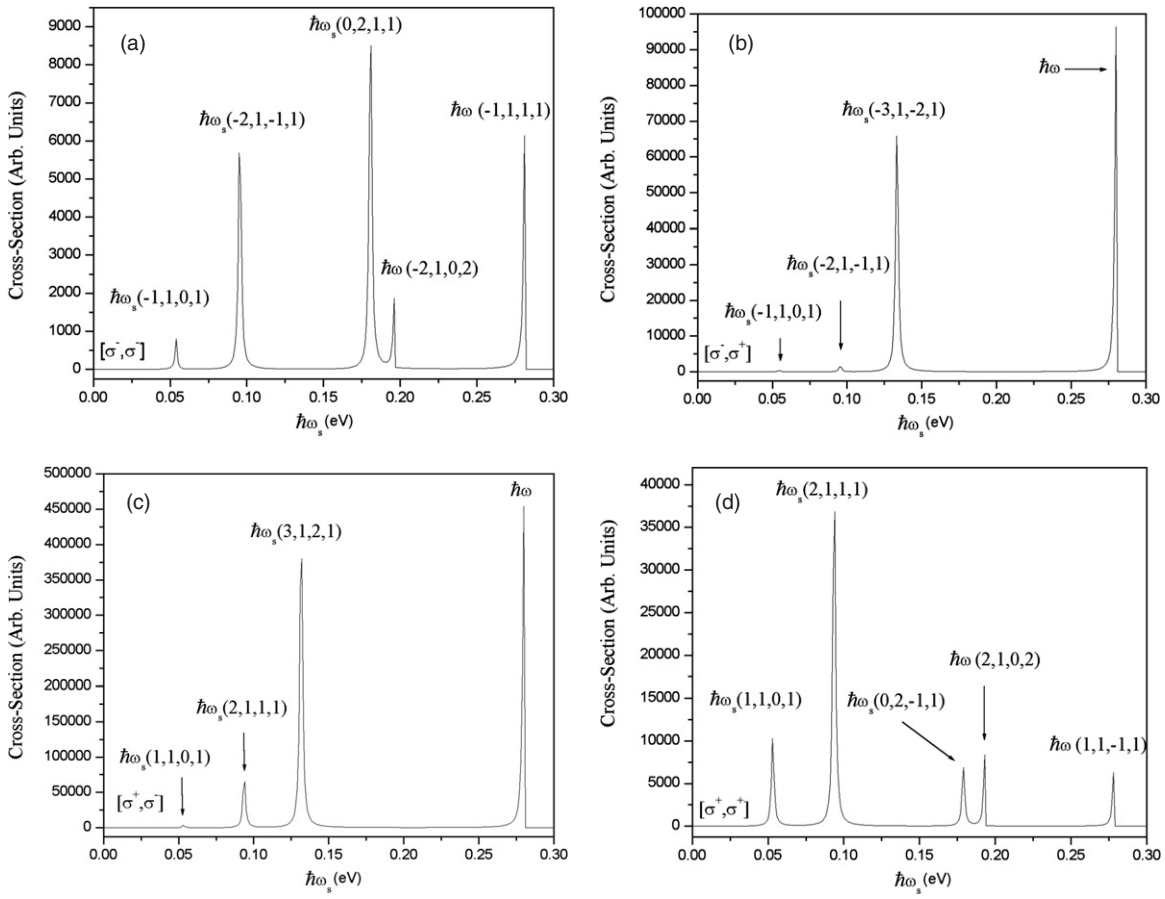

Figure 3. The emission spectra for a QWW for $\rho_0 = 60$ Å, $\hbar\omega_l = 0.28$ eV and $B_0 = 1$ T: (a) $[\sigma_s^- \cdot \sigma_l^-]$; (b) $[\sigma_s^- \cdot \sigma_l^+]$; (c) $[\sigma_s^+ \cdot \sigma_l^+]$ and (d) $[\sigma_s^+ \cdot \sigma_l^-]$.

the electron structure of the system. In a more realistic case we could consider a coupled band structure by using models like the Luttinger–Kohn or the Kane model. It can be easily proved that the singular peaks in the differential cross-section will be present independently of the model used for the subband structure and may be determined whenever the values of $\hbar\omega_s$ become equal to the *gap* between two subbands [24].

Acknowledgments

We are very grateful for the valuable comments made by the referees.

References

[1] Jusserand B and Cardona M 1989 *Light Scattering in Solids V* (*Springer Topics in Applied Physics* vol 66) ed M Cardona and G Güntherodt (Heidelberg: Springer)
[2] Kim N, Ihm G, Sim H-S and Chang K J 1999 *Phys. Rev.* B **60** 8767
[3] Barticevic Z, Pacheco M and Latgé A 2000 *Phys. Rev.* B **62** 6963
[4] Tan W-C and Inkson J C 1996 *Phys. Rev.* B **53** 6947
[5] Ismailov T G and Mehdiyev B H 2005 *Physica* E **31** 72
[6] Hashimzade F M, Ismailov T G, Mehdiyev B H and Pavlov S T 2005 *Phys. Rev.* B **71** 165331
[7] Hyun C Lee 1999 *Int. J. Mod. Phys.* B **13** 2275
[8] Kushwaha M S 2001 *Surf. Sci. Rep.* **41** 1
[9] Riera R, Marín J L and Rosas R A 2001 Optical properties and impurity states in nanostructured materials *Handbook of Advanced Electronic and Photonic Devices* vol 6, ed H S Nalwa (New York: Academic) chapter 6
[10] Betancourt-Riera R, Riera R, Marín J L and Rosas R A 2004 Electron Raman scattering in nanostructures *Encyclopedia of Nanoscience and Nanotechnology* vol 3 (Stevenson Ranch: American Scientific Publishers) pp 101–37
[11] Riera R, Comas F, Trallero-Giner C and Pavlov S T 1988 *Phys. Status Solidi* b **48** 533
[12] Bergues J M, Betancourt-Riera R, Marin J L and Riera R 1996 *Phys. Low-Dimens. Struct.* **7/8** 81
[13] Betancourt-Riera R, Bergues J M, Riera R and Marin J L 2000 *Physica* E **5** 204
[14] Betancourt-Riera R, Riera R, Rosas R and Marin J L 2003 *Phys. Low-Dimens. Struct.* **1/2** 125
[15] Betancourt-Riera R, Rosas R, Marín-Enriquez I, Riera R and Marin J L 2005 *J. Phys.: Condens. Matter.* **17** 4451
[16] Bergues J M, Betancourt-Riera R, Riera R and Marin J L 2000 *J. Phys.: Condens. Matter.* **12** 7983
[17] Comas F, Trallero-Giner C, Lang I G and Pavlov S T 1985 *Fiz. Tverd. Tela* **27** 57
Comas F, Trallero-Giner C, Lang I G and Pavlov S T 1985 *Sov. Phys.—Solid State* **27** 32 (Engl. Transl.)
[18] Wallis R F and Mills D L 1970 *Phys. Rev.* B **2** 3312
[19] Bechstedt F, Enderlein R and Peuker K 1975 *Phys. Status Solidi* b **68** 43
[20] Gadzhiev A T, Gashimzade F M and Mustafaev N B 1991 *J. Phys.: Condens. Matter.* **3** 4677

[21] Liu C-H, Ma B-K and Chen C-Y 2002 *Chin. Phys.* **9** 844
[22] Trallero-Giner C, Ruf T and Cardona M 1990 *Phys. Rev.* B **41** 3028
[23] Betancourt-Riera R, Rosas R, Marin-Enriquez I, Riera R and Marin J L 2005 *J. Phys.: Condens. Matter.* **17** 4451
[24] Comas F, Trallero Giner C and Perez-Alvarez R 1986 *J. Phys. C: Solid State Phys.* **19** 6479